On the dynamic behavior of the current in the condenser of a boost converter controlled with ZAD

Dario Del Cristo Vergara Perez[1], Simeon Casanova Trujillo[2], and Fredy E. Hoyos Velasco[3]
[1]Institución Educativa San Marcos, Colombia
[2]Universidad Nacional de Colombia, Sede Manizales,
Investigation Group: Scientific Calculation and Mathematical Modeling, Colombia
[3]Universidad Nacional de Colombia, Sede Medellín, Facultad de Ciencias, Escuela de Física, Colombia

Article Info	ABSTRACT
	In this paper, an analytical and numerical study is conducted on the dynamics of the current in the condenser of a boost converter controlled with ZAD, using a pulse PWM to the symmetric center. A stability analysis of periodic 1T-orbits was made by the analytical calculation of the eigenvalues of the Jacobian matrix of the dynamic system, where the presence of flip and Neimar–Sacker-type bifurcations was determined. The presence of chaos, which is controlled by ZAD and FPIC techniques, is shown from the analysis of Lyapunov exponents.

Corresponding Author:

Fredy E. Hoyos Velasco,
Sede Medellín, Facultad de Ciencias,
Universidad Nacional de Colombia,
Escuela de Física, Medellín, Carrera 65 No. 59A-110, Medellín, 050034, Colombia.
Email: fehoyosve@unal.edu.co

1. INTRODUCTION

DC-DC converters are devices that act as bridges for energy transfer between sources and loads, which leads to the question of how to transfer energy from a source with v_{in} amplitude to a load that needs v_{ref} voltage and with a minimum loss of power [1]. Among the multiple applications that these converters have been the power sources of computers, distributed power systems, and power systems in electric vehicles, aircraft, etc [2, 3]. Therefore, these converters have been a focus of research into the theories of dynamic systems. On the other hand, it has been established that around 90 % of electrical energy is processed through power converters before its final use [4]. There are different types of DC-DC converters, each with their own purpose. In some, the output voltage is higher than that of the input while in others it is lower. Currently, we have among others, boost, buck, and buck–boost converters [5, 6].

Of special interest is the boost converter [7], which is a voltage booster circuit that is widely used at the industrial level and that exhibits a nonlinear behavior by virtue of its switching system. Power converters, due to their configuration, can be seen as systems of variable structures [8, 9]. In the 1980s, drivers in sliding modes for this type of system began to be designed. However, this type of design has the disadvantage of generating "chattering" in the system, which increases ripple and distortion at the output [10].

In 2001, the ZAD control technique (zero average dynamic) was reported for the first time [11, 12]. This technique defines a switching surface and forces the dynamic system that governs the converter to evolve on that surface on average. This technique also guarantees a fixed switching frequency [13]. It is a design in which an auxiliary output is fixed and, based on this, it is defined which digital control action guarantees the average of the auxiliary output in each iteration [14]. The ZAD technique has been implemented in the buck converter and has shown good results in terms of robustness and low output error [15].

In [9], an analysis of the dynamics of a boost converter controlled with ZAD was conducted using the switching surface $s(x(t)) = k_1(x_1(t) - x_{1ref}) + k_2(x_2(t) - x_{2ref})$ and it was shown analytically that the approximation of the switching surface by straight lines is as good as desired. In other words, the error in the approximation can be made as small as we want; moreover, the maximum and minimum of the error in the approximation occur just at the ends of the sub-intervals, a fact that was corroborated by simulation in MATLAB. Another contribution that was obtained from this study is that the ZAD technique implemented in the boost converter presents good regulation due to the presence of zones in the bi parameter space $k_1 \times k_2$ in which the system regulates from 1% to 7%, being greater in the areas where regulation of 5% and 1% is presented. From these results, this article analyzes the dynamics of the current in the condenser of a boost converter controlled with the ZAD technique using a switching surface defined as a linear combination of the error in the voltage, error in the current, and the error in the condenser current as given by:

$$s(x(t)) = k_1(x_1(t) - x_{1ref}) + k_2(x_2(t) - x_{2ref}) + k_3(x_3(t) - x_{3ref})$$

2. MATHEMATICAL MODEL

The boost-type converter is a voltage booster circuit that uses the characteristics of the inductor and the capacitor as energy storage elements to raise the current coming from the power supply and then inject it into the condenser, thus producing higher voltage levels in the load than those of the source [16]. The basic scheme of a boost converter is shown in Figure 1, where v_{in} is the input voltage, i is the current in the inductance of the inductor L, S is the switch, D is the diode, C is the capacity of the condenser, and v is the voltage in the load.

The boost converter has two conduction modes, namely [7, 17]:
- Continuous conduction mode (CCM): if the MOSFET and the diode are in complementary conditions (S = ON, D = OFF or S = OFF, D = ON)
- Discontinuous conduction mode (DCM): if the current that flows through the diode becomes equal to zero when the converter is operating with u = 0, then the diode will stop driving (S = OFF, D = OFF).

The system of equations described by this converter is as follows:

$$\frac{dv}{dt} = \frac{-1}{RC}v + \frac{1}{C}i(1 - u), \tag{1}$$

$$\frac{di}{dt} = \frac{-1}{L}v(1 - u) + \frac{v_{in}}{L}. \tag{2}$$

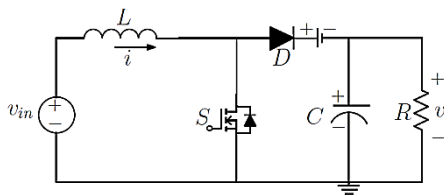Figure 2 shows the scheme of a boost converter considering the current i_C in the condenser C.

Figure 1. Scheme of a boost converter
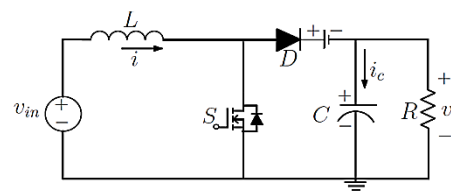
Figure 2. Schematic of a boost converter considering the current in condenser C

q, C, and $v_C = v$ represent the load, capacitance, and voltage in capacitor C, respectively. It is known that $q = C \cdot v_C$ (C is constant, while q and V_C depend on time). From this last equality we obtain

$$\frac{dq}{dt} = C \cdot \frac{dv_C}{dt}$$

as

$$\frac{dq}{dt} = i_C = i_C(t),$$

and therefore

$$i_C = C \cdot \frac{dv_C}{dt}. \tag{3}$$

On the other hand, because C and R are in parallel, v_C. Thus, replacing in (4) we obtain $i_C = C \cdot \frac{dv}{dt}$, where

$$\frac{1}{C} \cdot i_C = \frac{dv}{dt}. \tag{4}$$

$C \neq 0$ because we are working in continuous conduction mode using (4) and (5) as

$$\frac{1}{C} \cdot i_C = \frac{-1}{RC}v + \frac{1}{C}i(1-u),$$

where

$$i_C = \frac{-1}{R}v + i(1-u). \tag{5}$$

deriving (6) with respect to t, we have

$$\frac{di_C}{dt} = \frac{-1}{R}\frac{dv}{dt} + \frac{di}{dt}(1-u). \tag{6}$$

on the other hand, using (2) and (3) in (6) we obtain:

$$\frac{di_C}{dt} = \frac{1}{R^2C}v - \frac{1}{RC}i(1-u) + \left[\frac{v_{in}}{L} - \frac{1}{L}v(1-u)\right](1-u). \tag{7}$$

the system to be studied is:

$$\frac{dv}{dt} = \frac{-1}{RC}v + \frac{1}{C}i(1-u), \tag{8}$$

$$\frac{di}{dt} = \frac{-1}{L}v(1-u) + \frac{v_{in}}{L}, \tag{9}$$

$$\frac{di_C}{dt} = \frac{1}{R^2C}v - \frac{1}{RC}i(1-u) + \left[\frac{v_{in}}{L} - \frac{1}{L}v(1-u)\right](1-u). \tag{10}$$

Making the change of variables:

$$\tau = \frac{t}{\sqrt{LC}}, \ x_1 = \frac{v}{v_{in}}, \ x_2 = \sqrt{\frac{L}{C}}\frac{i}{v_{in}} \text{ and } x_3 = \frac{R}{v_{in}}i_C,$$

where τ is the new variable with respect to which the derivatives are going to be taken. Note that now x_3 is the dimensionless variable associated with the current in the condenser. Substituting in (9), we have

$$\frac{dv}{dt} = \frac{-1}{RC}v + \frac{1}{C}i(1-u)$$
$$\frac{v_{in}}{\sqrt{LC}}\frac{dx_1}{d\tau} = \frac{-1}{RC}v_{in}x_1 + \frac{1}{C}v_{in}x_2\sqrt{\frac{C}{L}}(1-u) \tag{11}$$
$$\frac{dx_1}{d\tau} = -\sqrt{\frac{L}{R^2C}}x_1 + x_2(1-u).$$

by doing $\gamma = \sqrt{\frac{L}{R^2C}}$, the system is as follows:

$$\dot{x}_1 = -\gamma x_1 + x_2(1-u)$$
$$\dot{x}_2 = -x_1(1-u) + 1$$
$$\dot{x}_3 = \gamma^{-1}(1-u)x_1 - \gamma x_3 + \gamma^{-1}(1-u).$$

the system is expressed matrixically as follows:

$$\begin{pmatrix} \dot{x}_1 \\ \dot{x}_2 \\ \dot{x}_3 \end{pmatrix} = \begin{pmatrix} -\gamma & (1-u) & 0 \\ (u-1) & 0 & 0 \\ \gamma^{-1}(1-u) & 0 & -\gamma \end{pmatrix}\begin{pmatrix} x_1 \\ x_2 \\ x_3 \end{pmatrix} + \begin{pmatrix} 0 \\ 1 \\ \gamma^{-1}(1-u) \end{pmatrix}.$$

in compact form, it is expressed as $\dot{x} = A_i x + B_i$, where i takes the value of 1 or 2. For $i = 1$, we take $u = 1$ and so

$$A_1 = \begin{pmatrix} -\gamma & 0 & 0 \\ 0 & 0 & 0 \\ 0 & 0 & -\gamma \end{pmatrix}, B_1 = \begin{pmatrix} 0 \\ 1 \\ 0 \end{pmatrix}.$$

for $i = 2$, we take $u = 0$ and so

$$A_2 = \begin{pmatrix} -\gamma & 1 & 0 \\ -1 & 0 & 0 \\ \gamma^{-1} & 0 & -\gamma \end{pmatrix}, B_2 = \begin{pmatrix} 0 \\ 1 \\ \gamma^{-1} \end{pmatrix}.$$

2.1. Pulse width modulation

When the PWM modulator (Pulse Width Modulation [18]) is applied as shown in Figure 3, u will be the control variable of the system and it will be specified in the following way:

$$u = \begin{cases} 1 & \text{if} & nT \le t \le nT + \frac{d}{2} \\ 0 & \text{if} & nT + \frac{d}{2} < t < (n+1)T - \frac{d}{2} \\ 1 & \text{if} & (n+1)T - \frac{d}{2} \le t \le (n+1)T \end{cases}. \tag{12}$$

2.2. Steady state duty cycle

In steady state, the input signal in the system follows the reference signal. For this work, the reference signal is constant and equal to the vector

$$\begin{pmatrix} x_{1ref} \\ x_{2ref} \\ x_{2ref} \end{pmatrix} = \begin{pmatrix} x_{1ref} \\ \gamma x_{1ref}^2 \\ \frac{x_{1ref}+1}{\gamma^2 x_{1ref}} \end{pmatrix}. \tag{13}$$

by replacing (14) in (17), we get the expression for the duty cycle d^* in steady-state:

$$d^* = \frac{T(x_{1ref}-1)}{x_{1ref}}. \tag{14}$$
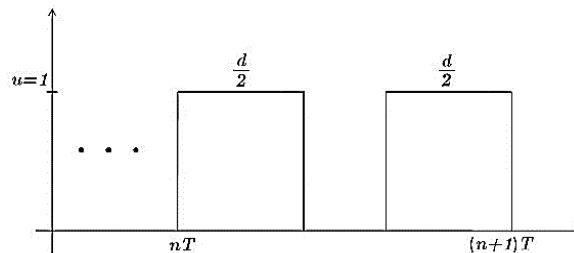

Figure 3. PWM modulator

3. CONTROL STRATEGY
3.1. ZAD control technique

With this technique, the duty cycle is calculated; that is, the time in which the switch is open or closed. This technique consists of the following [8, 19, 20]:
- Define a switching surface $s(x(t)) = 0$ in which the system will evolve on average
- Set a T period
- Impose that s have zero mean in each cycle:

$$\int_{nT}^{(n+1)T} s(x(t))dt = 0, \tag{15}$$

$$\begin{aligned} s(x(t)) &= k_1(x_1(t) - x_{1ref}) + k_2(x_2(t) - x_{2ref}) \\ &\quad + k_3(x_3(t) - x_{3ref}) \end{aligned}$$

The last condition guarantees that there will only be a finite number of commutations per period.

3.2. Calculation of the duty cycle

The duty cycle is calculated using the ZAD technique, approaching the switching surface by straight lines and using directly the equality $\int_{nT}^{(n+1)T} s\big(x(t)\big)dt = 0$. Solving the integral and equaling to zero and solving for d, we get that:

$$d_T = \frac{2s(x(nT)) + T\dot{s}_2(x(nT))}{\dot{s}_2(x(nT)) - \dot{s}_1(x(nT))},$$ (16)

where d_T is a real number between 0 and T. However,
−   if $d_T < 0$, then we force the system to evolve according to topology 1.
−   if $d_T > T$, then we force the system to evolve according to topology 2.
−   if the denominator of (16) is equal to zero, then we require the system to evolve according to topology 1 if the numerator $2s(x(nT)) + Ts_2(x(nT)) > 0$, and that it evolves according to topology 2 if $2s(x(nT)) + Ts_2(x(nT)) < 0$.

3.3. Lyapunov exponents

Lyapunov Exponents are a mathematical tool by means of which the speed of convergence or divergence of two orbits of a differential equation can be determined and whose initial conditions differ infinitesimally from one another [21, 22]. A Lyapunov exponent zero or negative indicates a strong relationship with the initial state and a direct dependence on it. However, a positive exponent indicates the existence of chaotic activity [23].
Definition 1
Let $DF(x)$ be the Jacobian matrix of the Poincaré application [24] associated with the system of equations that governs the converter and let $\lambda_i(DF(x))$ be the i-th eigenvalue of $DF(x)$. The Lyapunov exponent L_i for each eigenvalue is given by:

$$L_i = \lim_{n \to \infty} \left(\frac{1}{n} \sum_{k=0}^{n} log|\lambda_i(DF(x))| \right)$$ (17)

4. CHAOS

The term "chaos" was first formally introduced in mathematics by Li and Yorke; however, there is still no universally accepted or unified definition within the rigor of scientific literature [25]. Chaos is a word that originally denoted the complete lack of form or systematic organization, but now is often used to indicate the absence of a certain order. A more accepted definition is that of a long-term aperiodic behavior in a deterministic system and exhibits dependence sensitive to initial conditions. That is, it is an irregular behavior in which any variation in any initial condition can cause a drastic change in the evolution of the system as shown in Figure 4. For the study of chaos, we use the following definition [8].
Definition 2
A system is chaotic if it satisfies the following conditions:
−   Possesses positive Lyapunov exponents
−   Has a sensitive dependence on initial conditions in its domain
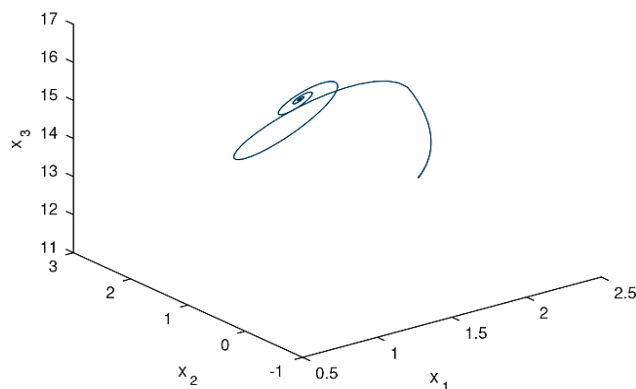−   It is bounded

Figure 4. Evolution of the system

4.1. Bifurcations

A bifurcation is a qualitative change of a dynamic system that occurs when one or more of the system parameters varies [26]. A dynamic system can have several stable equilibrium solutions. For a given set of parameters and an initial condition, the system converges to an equilibrium solution (attractor); however, if the parameters are varied, then it is possible that the equilibrium solution becomes unstable. A bifurcation diagram is a graph showing the behavior of the solutions of a long-term system when one or several parameters of the system are varied.

5. NUMERICAL RESULTS

5.1. Performance of the ZAD strategy with approach by straight lines to sections of the switching surface

Below are numerical results of the behavior of the variables of the state of the system and of the duty cycle when studying the dynamics of the boost converter considering the current in condenser C when applying the ZAD technique of the pulse to the symmetric center. The system is simulated while fixing the parameters $k_1, k_2, k_3, T = 0.18$, and $\gamma = 0.35$. In Figure (5), the values $k_1 = 1.5$, $k_2 = 0.5$, $k_3 = 0.5$, and $T = 0.18$ were taken. We can see that

$$|2.5000 - 1.0000| = 1.5000$$
$$|2.1875 - 0.3500| = 1.8375 \quad .$$
$$|11.4286 - 16.3265| = 1.8375$$

Whose relative errors are 60 % for the voltage and 84 % for the current and 42.85 % for the current in the condenser C, which allows us to say that the boost converter system does not have a good ability to follow the constant reference signal, considering the current in the condenser C.

5.2. Flip-type bifurcations

These orbits are given when the eigenvalue goes from being stable to unstable by crossing -1. This type of bifurcation is characterized by the fact that the $1T$-periodic orbit becomes unstable and a $2T$-periodic orbit is born; that is, a doubling period occurs [8]. Figure 6 shows a configuration of parameters where $\gamma = 0.35$, $T = 0.18$ s, with initial condition $(2.5, 2.1875, 11.4286)^T$, $k_1 = 0.5$, $k_2 = 0.5$, and the point of interest is found varying at $k_3 \in [-1.6, 0]$. From this figure, we see that the $1T$-periodic orbit loses its stability when $k_3 \approx -1.49$. When reviewing the eigenvalues of the Jacobian matrix as shown in Table 1, associated with the Poincaré application, it can be seen that the bifurcation obtained is of the flip type because for a value of the parameter $k_3 \approx -1.49$, it goes from being stable to unstable.
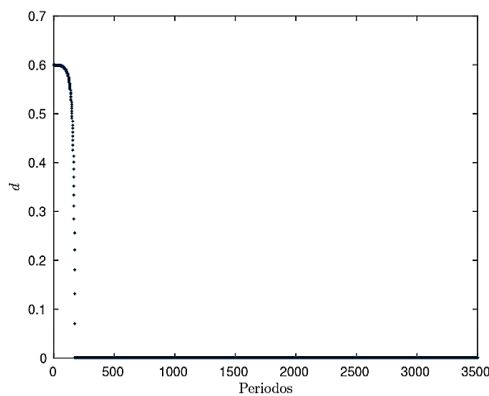

Figure 5. Behavior of regulation
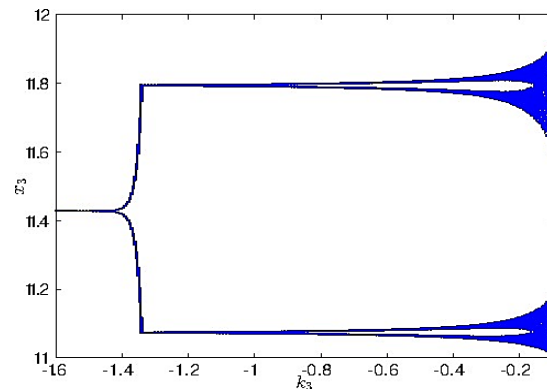
Figure 6. Bifurcation diagram of the current in the condenser as a function of k_3, $k_1 = 0.5$, and $k_2 = 0.5$

Table 1. Eigenvalues Associated with the Variation of k_3, $k_1 = 0.5$ and $k_2 = 0.5$

k_3	λ_1	λ_2	λ_3	ρ
-1.6000	**-0.9988**	**0.9067**	**0.9755**	**0.9988**
-1.2800	-1.0025	0.9051	0.9736	1.0025
-0.9600	-1.0087	0.9023	0.9708	1.0087
-0.6400	-1.0210	0.8961	0.9658	1.0210
-0.3200	-1.0578	0.8743	0.9560	1.0578
	0.9389	-3.3278	0.2891	3.3278

5.3. Neimar-Sacker-type bifurcations

This type of bifurcation is characterized specifically because when examining the evolution of the eigenvalues of the Jacobian matrix of the Poincaré map, these eigenvalues are complex and conjugated; in addition, the module approaches 1. Figure 7 shows a configuration of parameters $\gamma = 0.35$, $T = 0.18$ s and initial condition $(2.5, 2.1875, 11.4286)^T$, $k_1 = 0.5$, $k_2 = -0.5$, and the point of interest is found varying $k_3 \in [-0.204, -0.19]$. From this figure, we have that the $1T$-periodic orbit loses its stability when $k_3 \approx -0.193$. When reviewing the eigenvalues of the Jacobian matrix as shown in Table 2 associated with the Poincaré application, it is observed that the bifurcation obtained is of the Neimar–Sacker type because for a value of the parameter $k_3 \approx -0.193$, conjugated complex eigenvalues enter the unit circle.
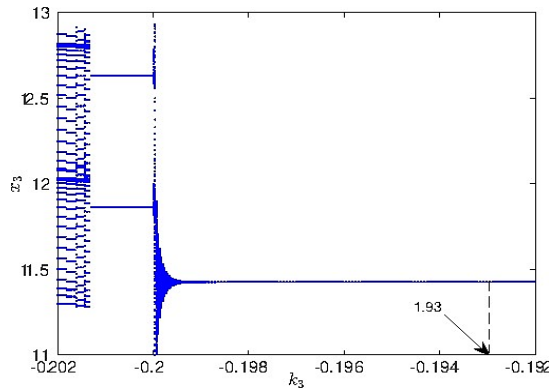

Figure 7. Bifurcation diagram of the current in the condenser as a function of k_3, $k_1 = 0.5$, and $k_2 = -0.5$

5.4. Presence of chaos

Figure 8 shows the presence of chaos in the boost converter when the current in condenser C is considered in the range $k_3 \in [-1.45, 0.027]$ due to the presence of positive Lyapunov exponents.
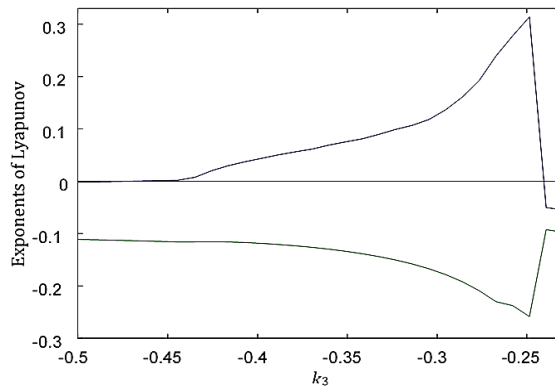

Figure 8. Variation of the Lyapunov exponents as a function of k_3, $k_1 = 0.5$, and $k_2 = 0.5$

Table 2. Eigen values associated with the variation of k_3, $k_1 = 0.5$, $k_2 = -0.5$

k_3	λ_1	λ_2	λ_3	ρ
-0.2200	$-0.7574 + 0.0000i$	$1.0789 + 0.0344i$	$1.0789 - 0.0344i$	1.0795
-0.1900	$-0.9031 + 0.0000i$	$0.9872 + 0.0551i$	$0.9872 - 0.0551i$	**0.9888**
-0.1600	$-0.9348 + 0.0000i$	$0.9711 + 0.0403i$	$0.9711 - 0.0403i$	0.9719
-0.1300	$-0.9487 + 0.0000i$	$0.9644 + 0.0296i$	$0.9644 - 0.0296i$	0.9648
-0.1000	$-0.9564 + 0.0000i$	$0.9607 + 0.0208i$	$0.9607 - 0.0208i$	0.9609

6.   CHAOS CONTROL WITH FPIC

In order to apply FPIC technique [20], we consider a discrete dynamic system described by a set of:

$$x_{k+1} = f\big(x_k, u(x_k)\big),$$

where $x_k \in \mathbb{R}^n, u \colon \mathbb{R}^n \to \mathbb{R}, f \colon \mathbb{R}^{n+1} \to \mathbb{R}^n$, suppose that the system has a fixed point

$$\left(x^*, u(x^*)\right) := (x^*, u^*).$$

When calculating the Jacobian of the system in this fixed point, we obtain $J = J_x + J_u$, where

$$J_x = \left(\frac{\partial f}{\partial x}\right)_{(x^*,u^*)} \quad and \quad J_u = \left(\frac{\partial f}{\partial u}\frac{\partial u}{\partial x}\right)_{(x^*,u^*)}.$$

If the spectral radius of J_x is less than one $(\rho(J_x) < 1)$, then there is a control signal

$$\hat{u}(k) = \frac{u(x(k)) + Nu^*}{N+1},$$

that guarantees the stability of the fixed point (x^*, u^*) for some $N \in \mathbb{R}^+$.

Considering the duty cycle of the system as the variable to be controlled, we modify the duty cycle as follows:

$$d(k) = \frac{d_T + Nd^*}{N+1}, \tag{18}$$

where $d(k)$ is the duty cycle to be applied, d_T is the duty cycle obtained in (17), d^* is the steady-state duty cycle (15), and N is a positive arbitrary constant.

Figure 9 shows that the FPIC technique is applicable to the system because the variation of the spectral radius in function of γ is less than 1 for different values of γ. When applying FPIC to the boost converter controlled with ZAD and considering the current in the condenser, in Figure 10 it is shown that when choosing $N = 0.01$, the range in which the system presents chaotic behavior is reduced for k_3 parameter. Figure 11 shows that by choosing $N = 0.04$, the range of chaotic behavior for k_3 parameter is further reduced.
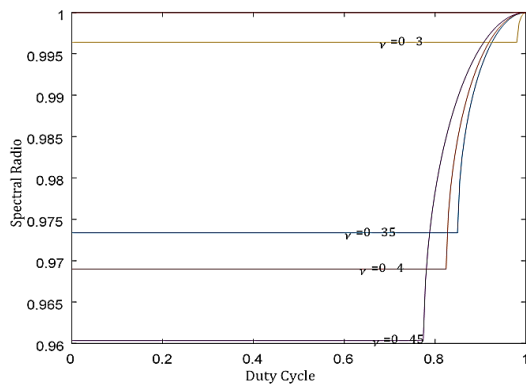

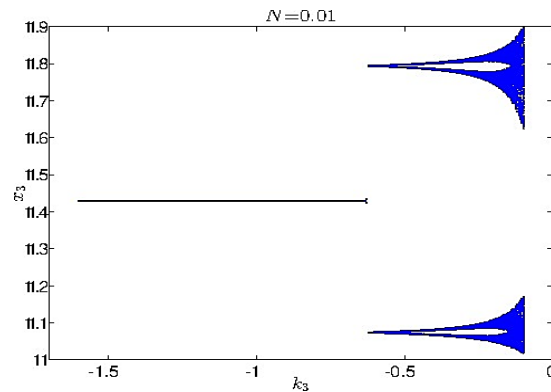Figure 9. Spectral radio as a function of γ

Figure 10. Voltage bifurcation diagram as a function of k_3 with $N = 0.01$
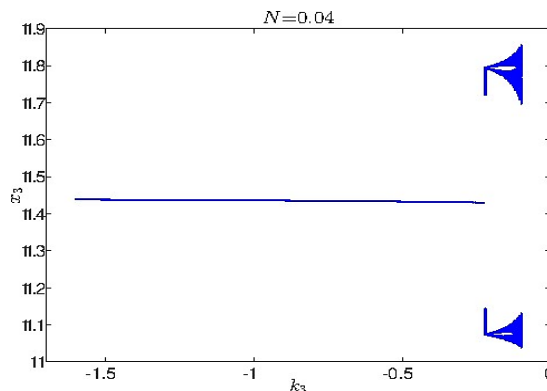

Figure 11. Voltage bifurcation diagram as a function of k_3 with $N = 0.04$

Figure 12 shows that when choosing $N = 0.06$, the chaos is almost completely reduced, which allows us to conclude that as we increase the value of the N constant of FPIC control, the zone of chaos of the system disappears. Figure 13 gives the levels in which the FPIC technique controls the chaos of the system. The blue color corresponds to areas where chaos is controlled and red corresponds to the presence of chaos. It is observed that for $N \approx 0.1155$, the chaos has already been completely eliminated for the set of considered values.
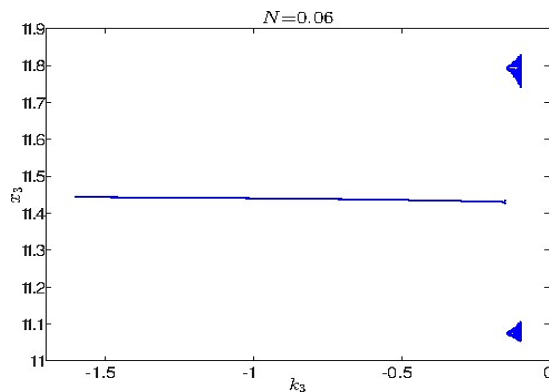

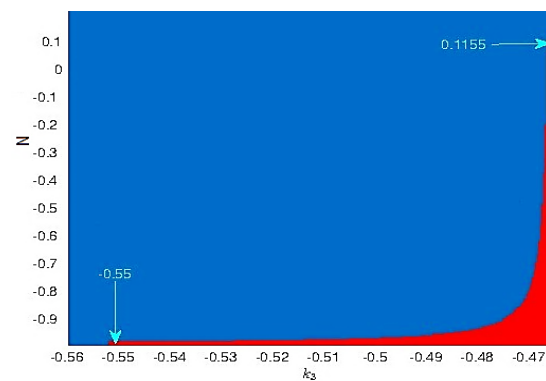Figure 12. Voltage bifurcation diagram as a function of k_3 with $N = 0.06$

Figure 13. Dimensions for the N constant of FPIC control

7.   CONCLUSIONS

The system of differential equations that governs the dynamics of a boost converter was obtained when the current in the condenser is considered. Additionally, the boost converter dynamics was made when considering a switching surface that is a function of the current in the condenser, and the stability of the $1T$-periodic orbit for the boost converter was determined when the current in the condenser is considered by the exponents of Lyapunov. The ZAD strategy allowed us to obtain an exact expression for the duty cycle, which facilitates a more precise analysis of the dynamics of the converter. The current in the condenser for the ZAD-controlled system presents complex dynamics such as the existence of Neimar–Sacker-type bifurcation and chaotic behavior, which are determined by the variation of the self-values of the Jacobian matrix and the Lyapunov exponents, respectively. The FPIC technique works properly when controlling system chaos, which is important when conducting an experimental prototype. By simulating the system with the FPIC technique, it was shown that the range of stability of the parameter associated with the current is wide.

REFERENCES
[1]   F. E. Hoyos, J. E. Candelo, and J. A. Taborda, "Selection and validation of mathematical models of power converters using rapid modeling and control prototyping methods," *Int. J. Electr. Comput. Eng.*, vol. 8, no. 3, pp. 1551-1568, June 2018,
[2]   D. Sattianadan, K. Saravanan, S. Murugan, N. Hari, and P. Venkadesh, "Implementation of quasi-z source inverter for grid connected PV based charging station of electric vehicle," *Int. J. Power Electron. Drive Syst.*, vol. 10, no. 1, pp. 366-373, 2019,
[3]   C. Mahmoudi, F. Aymen, and S. Lassaad, "Smart database concept for Power Management in an electrical vehicle," *Int. J. Power Electron. Drive Syst.*, vol. 10, no. 1, pp. 160-169, March 2019.
[4]   S. Banerjee and G. C. Verghese, "Nonlinear Phenomena in Power Electronics: Bifurcations, Chaos, Control, and Applications," IEEE, p. 472, 2001.
[5]   N. Mohan, T. M. Undeland, and W. P. Robbins, "Power electronics : converters, applications, and design," John Wiley & Sons, 2003.
[6]   N. Mohan, "Power electronics: a first course," Wiley, 2011.

[7]   M. W. Umar, N. Yahaya, and Z. Baharudin, "State-space averaged modeling and transfer function derivation of DC-DC boost converter for high-brightness led lighting applications," *TELKOMNIKA Telecommunication Computing Electronic Control*, vol. 17, no. 2, pp. 1006-1013, April 2019.

[8]   A. Amador, S. Casanova, H. A. Granada, G. Olivar, and J. Hurtado, "Codimension-Two Big-Bang Bifurcation in a ZAD-Controlled Boost DC-DC Converter," *Int. J. Bifurc. Chaos*, vol. 24, no. 12, p. 1450150, Dec 2014.

[9]   D. D. C. Vergara Perez, S. C. Trujillo, and F. E. Hoyos Velasco, "Period Addition Phenomenon and Chaos Control in a ZAD Controlled Boost Converter," *Int. J. Bifurc. Chaos*, vol. 28, no. 13, p. 1850157, Dec 2018.

[10]   A. Levant, "Principles of 2-sliding mode design," *Automatica*, vol. 43, no. 4, pp. 576–586, Apr 2007.

[11]   E. Fossas, R. Griño, and D. Biel, "Quasi-sliding control based on pulse width modulation, zero averaged dynamics and the L2 norm," *Advances in Variable Structure Systems*, pp. 335-344, 2000.

[12]   D. Biel, E. Fossas, R. Ramos, and A. Sudria, "Control Implementation Based on Zero Averaged Dynamics," *Proc. 40th IEEE Conf. Decis. Control*, pp. 1825-1830, 2001.

[13]   R. R. Ramos, D. Biel, E. Fossas, and F. Guinjoan, "A fixed-frequency quasi-sliding control algorithm: Application to power inverters design by means of FPGA implementation," *IEEE Trans. Power Electron.*, vol. 18, no. 1, pp. 344-355, 2003.

[14]   F. E. Hoyos Velasco, N. Toro-García, and Y. A. Garcés Gómez, "Adaptive Control for Buck Power Converter Using Fixed Point Inducting Control and Zero Average Dynamics Strategies," *Int. J. Bifurc. Chaos*, vol. 25, no. 04, pp. 1550049, Apr 2015.

[15]   Hoyos, Candelo-Becerra, and Hoyos Velasco, "Model-Based Quasi-Sliding Mode Control with Loss Estimation Applied to DC–DC Power Converters," *Electronics*, vol. 8, no. 10, pp. 1086, Sep 2019.

[16]   J. Munoz, G. Osorio, and F. Angulo, "Boost converter control with ZAD for power factor correction based on FPGA," in *2013 Workshop on Power Electronics and Power Quality Applications (PEPQA)*, 2013, pp. 1-5, 2013.

[17]   R. Palanisamy, K. Vijayakumar, V. Venkatachalam, R. M. Narayanan, D. Saravanakumar, and K. Saravanan, "Simulation of various DC-DC converters for photovoltaic system," *Int. J. Electr. Comput. Eng.*, vol. 9, no. 2, pp. 917, Apr 2019.

[18]   M. H. Rashid, "Power electronics handbook : devices, circuits, and applications," Butterworth-Heinemann, 2011.

[19]   D. Biel, R. Cardoner, and E. Fossas, "Tracking Signal in a Centered Pulse ZAD Power Inverter," *International Workshop on Variable Structure Systems*, pp. 104-109, 2006.

[20]   F. Hoyos Velasco, J. Candelo-Becerra, and A. Rincón Santamaría, "Dynamic Analysis of a Permanent Magnet DC Motor Using a Buck Converter Controlled by ZAD-FPIC," *Energies*, vol. 11, no. 12, pp. 3388, Dec 2018.

[21]   A. Sambas, S. Vaidyanathan, M. Mamat, M. A. Mohamed, and M. S. WS, "A New Chaotic System with a Pear-shaped Equilibrium and its Circuit Simulation," *Int. J. Electr. Comput. Eng.*, vol. 8, no. 6, pp. 4951-4958, Dec 2018.

[22]   W. C. Y. Chan and C. K. Tse, "Study of bifurcations in current-programmed DC/DC boost converters: from quasiperiodicity to period-doubling," *IEEE Trans. Circuits Syst. I Fundam. Theory Appl.*, vol. 44, no. 12, pp. 1129-1142, 1997.

[23]   Wang Liqing and Wei Xueye, "Computation of Lyapunov exponents for a current-programmed buck boost converter," *The 2nd International Workshop on Autonomous Decentralized System 2002,* pp. 273-276, 2002.

[24]   A. El Aroudi, D. Giaouris, H. H.-C. Iu, and I. A. Hiskens, "A Review on Stability Analysis Methods for Switching Mode Power Converters," *IEEE J. Emerg. Sel. Top. Circuits Syst.*, vol. 5, no. 3, pp. 302-315, Sep 2015.

[25]   Guanrong Chen, "Control and anticontrol of chaos," in *1997 1st International Conference, Control of Oscillations and Chaos Proceedings (Cat. No.97TH8329)*, vol. 2, pp. 181-186, 1997. doi: 10.1109/COC.1997.631323.

[26]   M. F. P. Polo and M. P. Molina, "Chaotic and steady state behaviour of a nonlinear controlled gyro subjected to harmonic disturbances," *Chaos, Solitons & Fractals*, vol. 33, no. 2, pp. 623-641, Jul 2007.